

# Acid-Catalyzed Trimerization of Acetaldehyde: A Highly Selective and Reversible Transformation at Ambient Temperature in a Zeolitic Solid

Sang-Ok Lee, Simon J. Kitchin, and Kenneth D. M. Harris\*

School of Chemistry, University of Birmingham, Edgbaston, Birmingham B15 2TT, United Kingdom

Gopinathan Sankar, Markus Dugal, and John Meurig Thomas\*

Davy Faraday Research Laboratory, The Royal Institution, 21 Albemarle Street, London W1X4BS, United Kingdom

Received: June 26, 2001; In Final Form: October 15, 2001

Acetaldehyde is shown to undergo a reversible Brønsted acid-catalyzed cyclotrimerization reaction, with 100% selectivity, at ambient temperature within the zeolite host material ferrierite. It is shown by *in situ* solid-state  $^{13}\text{C}$  NMR spectroscopy and other techniques that the cyclic trimer is the only product formed in this reaction. The equilibrium proportions of acetaldehyde and the cyclic trimer at ambient temperature correspond to a conversion greater than 90%. In contrast, in the corresponding acid-catalyzed transformation of acetaldehyde in the liquid state, a broad distribution of products is obtained. The reversibility of the cyclotrimerization reaction in ferrierite is confirmed from the fact that, on adsorption of a pure sample of the cyclic trimer within ferrierite, a reaction occurs to produce acetaldehyde as the only product with the same equilibrium distribution of the cyclic trimer and acetaldehyde as that obtained from the reaction of acetaldehyde in ferrierite. The role of Brønsted acid catalysis in the transformation between acetaldehyde and the cyclic trimer in ferrierite is confirmed from the fact that no reaction occurs on adsorption of acetaldehyde within sodium-exchanged ferrierite.

## 1. Introduction

Concepts of catalysis arise in many diverse areas of chemical, biological, and materials sciences, and a worthwhile goal is to seek to establish a fundamental understanding of the unifying features that link different types of catalytic systems and processes. As a starting point, we require to define systems and processes that are chemically related, have sufficient structural similarities, and can be carried out under comparable experimental conditions. Zeolitic materials and other microporous solids are utilized in a wide variety of catalytic applications,<sup>1–5</sup> many of which rely on the Brønsted acidity of the framework and/or the geometric constraints imposed upon the reaction by the framework (i.e. shape selectivity). However, most catalytic applications of these materials are investigated at elevated temperatures (recalling that these framework structures may be stable up to temperatures of the order of 1000 °C in some cases), involving irreversible transformations to produce some desired product. In this study, we focus instead on acid-catalyzed reactions that occur at ambient temperature, with a view to exploring possible parallels with the wide range of acid-catalyzed transformations that are known to occur for organic molecules in the liquid state around ambient temperature. In addition, it is relevant to recall that the analogy<sup>3,4,6–11</sup> between the mode of action of enzymes and zeolites (as well as other molecular sieve catalysts such as metal-substituted aluminophosphates) requires the study of chemical transformations close to ambient temperature, corresponding to the temperatures at which enzyme-catalyzed processes occur in living systems.

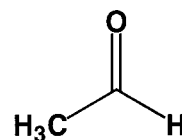


Figure 1. Molecular structure of acetaldehyde.

In pursuing these analogies, and focusing on acid-catalyzed transformations that occur under ambient conditions, model reaction systems include unimolecular rearrangements (following protonation), interconversions between tautomeric forms, and simple reactions involving nucleophilic substitution (either for the protonated reactant or the species produced following an initial rearrangement of the protonated reactant). Ideally, the model reaction system should have the potential to undergo a variety of competing reaction pathways, allowing selectivity to be probed. Despite the wide-ranging studies of catalytic applications of zeolitic materials, comparatively few studies of reactions under ambient conditions have been reported, with representative examples given in refs 12–20.

In this paper, we report a reversible acid catalyzed transformation that occurs at ambient temperature within a zeolitic solid and proceeds with substantially greater selectivity than the corresponding transformation under comparable conditions in the liquid state. We also discuss in more general terms the approaches and strategies that should be adopted in addressing relevant issues in this area.

The model reaction identified in this study is the transformation of acetaldehyde (Figure 1) within the zeolite host material ferrierite (Figure 2). The ferrierite structure<sup>21</sup> contains two types of tunnels (with cross sections  $4.2 \text{ \AA} \times 5.4$  and  $3.5 \text{ \AA} \times 4.8 \text{ \AA}$ ), both of which are accessible (as verified by molecular

\* To whom correspondence should be addressed. E-mail: K.D.M.H., K.D.M.Harris@bham.ac.uk; J.M.T., jmt@ri.ac.uk.

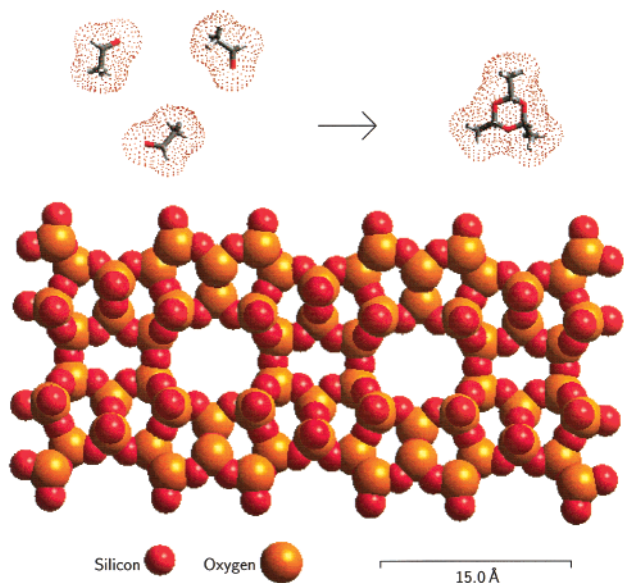


**Figure 2.** Computer graphic picture showing the structure of ferrierite viewed along the direction of the main tunnel. Three molecules of acetaldehyde and one molecule of the cyclic trimer **P** are shown, with molecular surfaces represented.

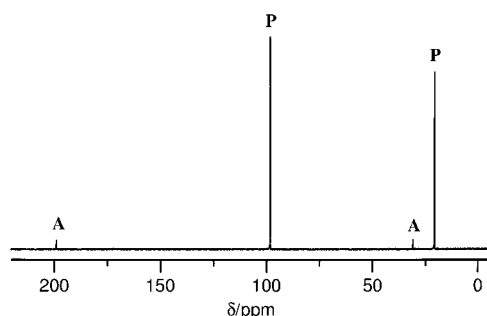


**Figure 3.** In situ high-resolution solid-state  $^{13}\text{C}$  NMR spectrum recorded at ambient temperature for a sealed ampule of acetaldehyde/ferrierite. Peaks due to acetaldehyde (denoted **A**) and the product **P** are marked.

modeling investigations carried out as part of this study) by molecules of the size of acetaldehyde. At ambient temperature, pure acetaldehyde is a stable liquid; in acidic environments, it is protonated on the oxygen atom of the carbonyl group, and a variety of competing processes may then ensue, as discussed below.

## 2. Results and Discussion

Acetaldehyde was included within the  $\text{H}^+$  form of ferrierite using the procedure described in section 4.2, followed by in situ characterization at ambient temperature using high-resolution solid-state  $^{13}\text{C}$  NMR spectroscopy (for the sample of acetaldehyde/ferrierite contained in a sealed quartz ampule). From the solid-state  $^{13}\text{C}$  NMR spectrum (Figure 3), it is clear that a reaction occurs to generate a single product (denoted **P**), together with some unreacted acetaldehyde. The product **P** is identified as the cyclic trimer shown in Figure 4. As discussed in section 4.4, this assignment was further confirmed from studies involving an authentic sample of pure **P** obtained commercially. A proposed mechanism for the Brønsted acid-catalyzed conversion of acetaldehyde to **P** is given in Figure 5.

We note that all lines in the solid-state  $^{13}\text{C}$  NMR spectrum of acetaldehyde/ferrierite (and those of the other samples discussed below) are very narrow. The fact that single narrow

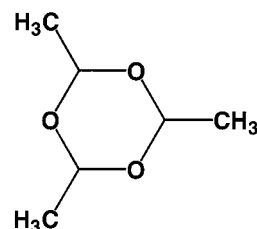


**Figure 4.** Molecular structure of the cyclic trimer **P**.

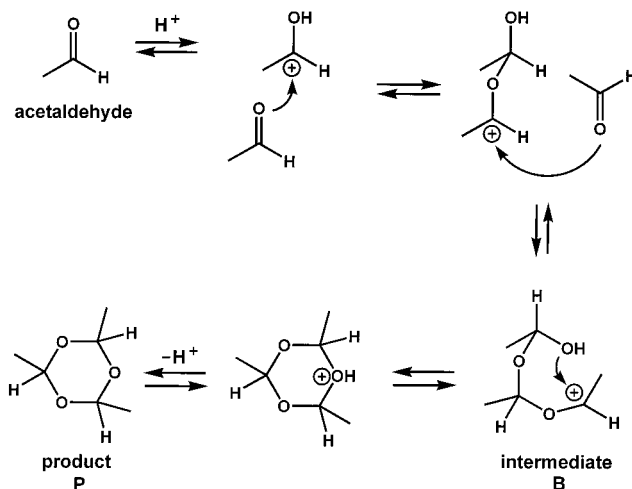


**Figure 5.** Proposed mechanism for the Brønsted acid-catalyzed cyclotrimerization of acetaldehyde to produce **P**.

lines are observed for both the methyl carbon and the ring carbon of **P** suggests that only one configurational isomer of **P** is produced, as elaborated in ref 24. As discussed below, this conclusion is further supported by results from solution state NMR studies.

From integration of the signals due to **P** and acetaldehyde in the solid-state  $^{13}\text{C}$  NMR spectrum, the percentage conversion from acetaldehyde to **P** in ferrierite at ambient temperature is estimated to be 93%, corresponding to a molar ratio of **P**:acetaldehyde of 4.43 (see ref 25). There was no change in the relative amounts of acetaldehyde and **P** during successive measurements of the solid-state  $^{13}\text{C}$  NMR spectrum, indicating that the reaction had already reached final conversion by the time of starting the solid-state NMR experiments. Thus, with the experimental approach used here, kinetic aspects of the reaction could not be investigated.

To further characterize the reaction product, the quartz ampule used in the solid-state  $^{13}\text{C}$  NMR experiments was broken under a nitrogen atmosphere, and the organic guest component inside the ferrierite was washed out with DMSO and studied by solution-state  $^1\text{H}$  and  $^{13}\text{C}$  NMR spectroscopy and GC-MS analysis. All analyses carried out indicated that acetaldehyde and **P** were the only species extracted from the ferrierite (see Figure 6a). From integration of the signals due to **P** and acetaldehyde in the solution-state  $^1\text{H}$  NMR spectrum, the percentage conversion from acetaldehyde to **P** was estimated to be 87%, in close agreement with the results from our solid-state NMR studies. In further agreement with the solid-state NMR results, our solution-state  $^1\text{H}$  and  $^{13}\text{C}$  NMR spectra support our assignment that only one configurational isomer of **P** is produced from the reaction of acetaldehyde in ferrierite (see ref 24).

In principle, linear oligomers  $[-\text{OCH}(\text{CH}_3)-]_n$  (with  $n > 3$ ) could also arise if the intermediate **B** in Figure 5 were to react with another monomer of acetaldehyde rather than undergoing

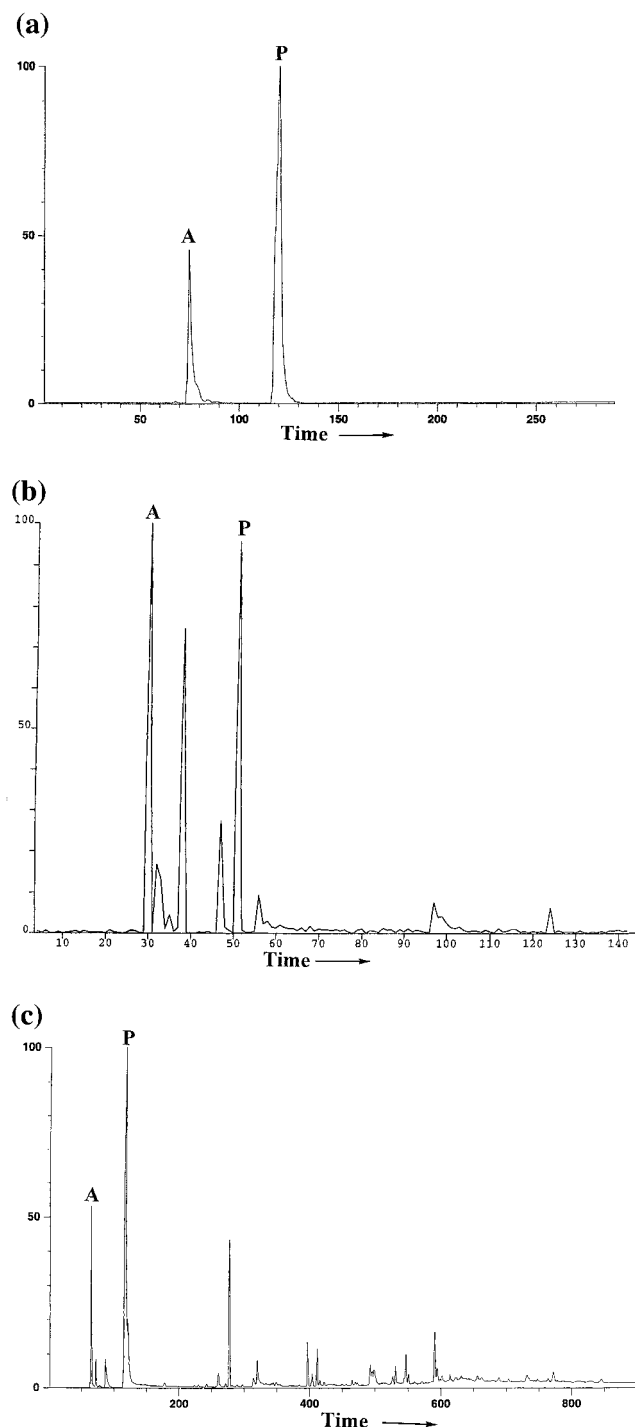


**Figure 6.** Comparison of gas chromatograms for the products from (a) the reaction of acetaldehyde in ferrierite (A = acetaldehyde; P = product), (b) the liquid-state reaction of acetaldehyde with *p*-toluenesulfonic acid, and (c) the liquid-state reaction of acetaldehyde with hydrochloric acid.

cyclization to produce **P**, but our GC-MS analysis of the guest species extracted from the ferrierite rules out the presence of any reaction product of mass higher than **P**. Furthermore, while the  $^1\text{H}$  and  $^{13}\text{C}$  chemical shifts in **P** may be rather close to those in linear oligomers, the signals due to the end groups in any oligomeric species would be observable in both the solid-state and solution-state NMR spectra (provided the number of monomer units  $n$  is not sufficiently high).

On a similar basis, the cyclic trimer shown in Figure 4 can be distinguished from the linear trimer, which would be produced by chain termination of the intermediate **B** in Figure

5. Clearly the linear trimer would contain more than one distinguishable  $\text{CH}_3$  carbon environment and more than one distinguishable  $\text{CH}$  carbon environment, which should be resolved in both the solid-state and solution-state NMR spectra.

Finally, a solid-state  $^{13}\text{C}$  NMR spectrum was recorded for the ferrierite sample after the extraction procedure with DMSO. The spectrum showed no evidence for any carbon-containing species (e.g. polymer) remaining behind in the ferrierite, confirming that all reaction products had been extracted.

To provide a comparison between the reaction of acetaldehyde in the constrained environment of the ferrierite host structure and the corresponding reaction of acetaldehyde in the liquid state, a number of control experiments were carried out. First, a small amount of *p*-toluenesulfonic acid was added to pure liquid acetaldehyde at ambient temperature (see section 4.5), and the mixture was studied subsequently by solution-state  $^1\text{H}$  and  $^{13}\text{C}$  NMR spectroscopy and GC-MS analysis. These analyses indicate that acetaldehyde reacts under these conditions in the liquid state to generate a substantial number of products, including the cyclic trimer **P**. In the solution-state  $^1\text{H}$  and  $^{13}\text{C}$  NMR spectra, the main peaks are in the region of the peak positions characteristic of the cyclic trimer **P** but are significantly broader than the peaks in the solution-state  $^1\text{H}$  and  $^{13}\text{C}$  NMR spectra for the products extracted from the reaction of acetaldehyde in ferrierite, showing that the liquid-state reaction generates a distribution of products with rather similar chemical environments. In this regard, we recall that the set of  $^1\text{H}$  and  $^{13}\text{C}$  chemical shifts for linear oligomers  $[-\text{OCH}(\text{CH}_3)-]_n$  of different chain length  $n$  and for cyclization products (such as **P**) should be close to each other due to the similarity of the local environments of a given type of functional group in each of these molecules. In addition, the solution-state  $^1\text{H}$  and  $^{13}\text{C}$  NMR spectra contain several peaks of comparatively low intensity at other positions, representing other minor products and/or end-group environments. In Figure 6, the gas chromatogram for the products from the liquid-state reaction (Figure 6b) is compared with that for the products extracted following the reaction of acetaldehyde in ferrierite (Figure 6a).

Another liquid-state reaction was carried out by adding a small amount of hydrochloric acid to liquid acetaldehyde at ambient temperature. Analysis by GC-MS (Figure 6c) and solution-state  $^1\text{H}$  and  $^{13}\text{C}$  NMR spectroscopy led to similar conclusions to those discussed above for the liquid-state reaction involving acetaldehyde and *p*-toluenesulfonic acid. In summary, it is clear that the reaction of acetaldehyde under conditions of Brønsted acidity in the liquid state generates a wide range of products, in contrast to the clear selectivity observed for the reaction of acetaldehyde in ferrierite.

Two additional investigations were carried out to understand further the nature of the reaction of acetaldehyde to produce **P** within the ferrierite host structure. First, to confirm that Brønsted acid catalysis is an essential feature of the reaction, we repeated our experiment within a sample of sodium-exchanged ferrierite, which is devoid of Brønsted acid sites (see section 4.6). The solid-state  $^{13}\text{C}$  NMR spectrum (Figure 7) recorded for this sample reveals that only unreacted acetaldehyde is present, with no detectable amounts of **P** or any other reaction product.

Second, after **P** was identified as the only product of the reaction in ferrierite, a sample of pure **P** (commercial name: paraldehyde) was obtained. To assess whether the transformation of acetaldehyde to **P** within ferrierite is genuinely reversible, the sample of pure **P** was adsorbed within ferrierite (see section 4.4), using the same procedure as that for the adsorption of acetaldehyde inside ferrierite. The solid-state  $^{13}\text{C}$  NMR spectrum

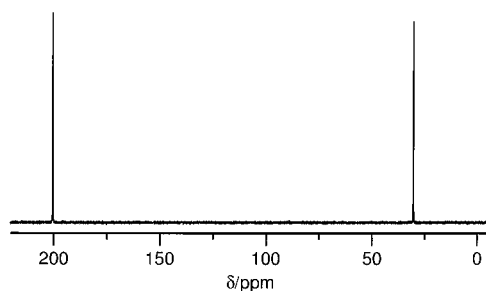


**Figure 7.** In situ high-resolution solid state  $^{13}\text{C}$  NMR spectrum recorded at ambient temperature for a sealed ampule containing the sample of acetaldehyde adsorbed in sodium-exchanged ferrierite.

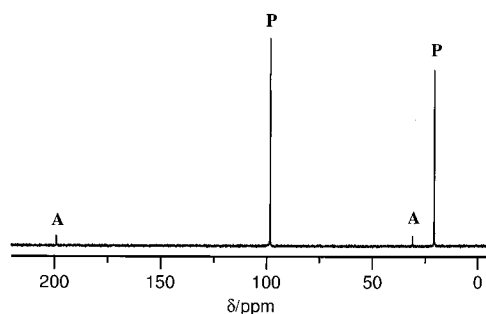


**Figure 8.** In situ high-resolution solid-state  $^{13}\text{C}$  NMR spectrum recorded at ambient temperature for a sealed ampule containing the sample of **P** adsorbed in ferrierite. Peaks due to acetaldehyde (denoted **A**) and **P** are marked.

(Figure 8) recorded at ambient temperature for a sealed quartz ampule containing this sample indicates that a reaction occurs to produce acetaldehyde and that acetaldehyde and **P** are the only organic species present. Importantly, the solid-state  $^{13}\text{C}$  NMR spectrum (Figure 8) is essentially identical to that (Figure 3) recorded for the sample prepared by adsorption of acetaldehyde inside ferrierite, and the relative proportions of acetaldehyde and **P** determined from these spectra are the same within experimental errors. The relative amounts of acetaldehyde and **P** (estimated by integration of the solid-state  $^{13}\text{C}$  NMR spectrum<sup>25</sup>) represent a percentage conversion (from acetaldehyde to **P**) of 92%, corresponding to a **P**:acetaldehyde molar ratio of 3.83. Thus, as expected from the principle of microscopic reversibility, the same equilibrium distribution of acetaldehyde and **P** is produced whether starting from pure acetaldehyde or starting from pure **P**. In this regard, we recall that each step in the proposed mechanism (Figure 5) for the acid-catalyzed interconversion between acetaldehyde and **P** is a reversible one.

### 3. Concluding Remarks

In this paper, we have identified a reaction that proceeds reversibly and with very high selectivity within a zeolitic host structure under ambient conditions. The high product specificity (in contrast to the corresponding reaction in the liquid state) is clearly a consequence of the spatial constraints imposed by the well-defined microenvironment within the zeolitic host structure.

In view of the wide range of acid catalyzed rearrangements of organic molecules known to occur in the solution state around ambient temperature, there are interesting opportunities to explore the effects of imposing spatial restrictions on these reactions by carrying them out within microporous Brønsted acid catalysts containing microenvironments of differing geometries. Furthermore, there is also scope to “tune” the positioning of active sites within these inorganic microporous

catalysts, as demonstrated<sup>22,23</sup> in the regioselective oxidation of alkanes, to further impose geometric specificity over organic transformations occurring within them.

## 4. Experimental Section

**4.1. Instrumentation.** All solid-state  $^{13}\text{C}$  and  $^1\text{H}$  NMR spectra were recorded using a Chemagnetics CMX Infinity 300 spectrometer, at 75.49 and 300.18 MHz respectively.

Solution-state  $^{13}\text{C}$  NMR spectra were recorded at 75.49 MHz on a Bruker AC300 spectrometer using  $\text{DMSO}-d_6$  as solvent and a PENDANT pulse sequence. Solution-state  $^1\text{H}$  NMR spectra were recorded at 300.18 MHz on a Bruker AC300 spectrometer using  $\text{DMSO}-d_6$  as solvent.

Thermogravimetric analysis was carried out using a Perkin-Elmer TGA6 instrument under a flow of nitrogen gas, with the sample heated from 30 to 600 °C at a rate of 10 °C  $\text{min}^{-1}$ .

GC-MS analysis was carried out using a VG Prospec mass spectrometer equipped with a Fisons 8000 series gas chromatograph. The samples were injected into a 25 m DB5 capillary column and separated using a temperature program from 60 to 250 °C at 10 °C  $\text{min}^{-1}$ .

**4.2. Preparation of Acetaldehyde/Ferrierite.** A sample of ferrierite (idealized formula  $\text{Na}_2\text{Mg}_2[\text{Al}_6\text{Si}_3\text{O}_{72}]\cdot 18\text{H}_2\text{O}$ ) with an actual Si/Al ratio of 40 was calcined in air at 550 °C for 12 h and dehydrated under vacuum at 400 °C for 1 h. Using standard vacuum line techniques, acetaldehyde was adsorbed from the gas phase into the dehydrated ferrierite, which was contained in a 9.5 mm diameter quartz tube. The temperature of the acetaldehyde/ferrierite sample was not raised above ambient temperature during this procedure. After adsorption, the quartz tube was immersed in liquid nitrogen and sealed to form an ampule of appropriate length for solid-state NMR experiments. In a separate series of thermogravimetric analysis experiments, the loading of acetaldehyde in the ferrierite was estimated to represent approximately 5.3 molecules of acetaldehyde per unit cell of ferrierite.

**4.3. Analysis of Acetaldehyde/Ferrierite.** Solid-state  $^{13}\text{C}$  NMR spectra were recorded at ambient temperature (25 °C) on the sealed quartz ampule of acetaldehyde/ferrierite, which was wrapped in PTFE tape to ensure a tight fit within the magic-angle spinning NMR rotor (9.5 mm diameter). The spectra were recorded using a direct polarization spin-echo sequence (to suppress the signal from the PTFE tape), under conditions of magic-angle spinning and  $^1\text{H}$  decoupling. The magic angle spinning frequency was 1.0 kHz (stable spinning at higher frequencies was difficult to attain for the sealed ampules, although the comparatively low spinning frequency used has no detrimental effect on the quality of the spectra recorded).  $^1\text{H}$  decoupling was carried out using the WALTZ sequence and was applied during acquisition and during the spin-echo delays but not during the recycle delay. We note that, for the samples studied here, high-power (16 kHz) CW decoupling was not able to completely remove the  $^{13}\text{C}-^1\text{H}$   $J$ -coupling. The recycle delay was 30 s.

Following the solid-state NMR experiments, the ampule was broken in an atmosphere of dry nitrogen (glovebox) and the organic species present within the ferrierite were extracted in DMSO. These extracts were analyzed by solution-state  $^1\text{H}$  and  $^{13}\text{C}$  NMR spectroscopy and GC-MS analysis. The results of these analyses confirm the assignment of the cyclic trimer **P** as the only reaction product (in addition to unreacted acetaldehyde).

**4.4. Preparation and Analysis of P/Ferrierite.** After identification of **P** as the only product from the reaction of acetaldehyde in ferrierite, a sample of pure **P** (paraldehyde) was

obtained from Sigma-Aldrich. First, solution-state  $^1\text{H}$  and  $^{13}\text{C}$  NMR spectra were recorded for the sample of pure **P** and confirmed that the product from the reaction of acetaldehyde in ferrierite had been correctly assigned as **P**.

Second, the sample of pure **P** was adsorbed inside ferrierite using the procedure described (for acetaldehyde) in section 4.2. The solid-state  $^{13}\text{C}$  NMR spectrum of a sealed quartz ampule containing the sample of **P**/ferrierite was recorded at ambient temperature using the procedure described in section 4.3. Following the solid-state NMR experiment, the ampule was broken in an atmosphere of dry nitrogen (glovebox) and the organic species present within the ferrierite were extracted in DMSO. These extracts were analyzed by solution-state  $^1\text{H}$  and  $^{13}\text{C}$  NMR spectroscopy and GC-MS analysis, as described in section 4.3.

**4.5. Reaction of Acetaldehyde in the Liquid State.** To investigate the behavior of acetaldehyde in the presence of Brønsted acids in the liquid state, small amounts of *p*-toluenesulfonic acid and hydrochloric acid were added (in separate experiments) to acetaldehyde (10 mL) and left at ambient temperature for 10 h. Each mixture was then studied by solution-state  $^{13}\text{C}$  and  $^1\text{H}$  NMR spectroscopy and GC-MS analysis.

**4.6. Experiments on Sodium-Exchanged Ferrierite.** To confirm the role of Brønsted acid catalysis in the reaction observed for acetaldehyde in ferrierite, an experiment was carried out involving adsorption of acetaldehyde within a sample of sodium-exchanged ferrierite. To prepare sodium-exchanged ferrierite, a sample of the  $\text{H}^+$  form of ferrierite (6 g) was added to 1.5 L of aqueous sodium acetate (0.1 M), and the solution was stirred overnight. The ferrierite was then filtered off, washed with water, and dried in an oven at 100 °C for 3 h. The procedures described in section 4.2 for calcination and dehydration of ferrierite were carried out. A solid-state  $^1\text{H}$  NMR spectrum recorded for the sample of sodium-exchanged ferrierite contained in a sealed quartz ampule showed that no detectable amounts of Brønsted acid sites were present [this spectrum was recorded using a single  $^1\text{H}$  pulse sequence with magic-angle spinning (spinning frequency 2.5 kHz; rotor diameter 9.5 mm; recycle delay 30 s)].

Acetaldehyde was adsorbed within the sample of sodium-exchanged ferrierite using the procedure described in section 4.2. Analysis of the resulting material by solid-state  $^{13}\text{C}$  NMR spectroscopy (using the procedure described in section 4.3) confirmed that no reaction had occurred (i.e. acetaldehyde was detected as the only organic species present within the ferrierite).

**Acknowledgment.** Financial support from EPSRC (to J.M.T.), HEFCE and EPSRC (to K.D.M.H.), and the University of Birmingham and CVCP (award of a studentship to S.O.L.) is gratefully acknowledged.

## References and Notes

- (1) John, C. S.; Clark, D. M.; Maxwell, I. E. In *Perspectives in Catalysis*; Thomas, J. M., Zamarayev, K. I., Eds.; Blackwell: Oxford, U.K., 1992; p 387.
- (2) Van Bekkum, H.; Flanigen, E. M.; Jansen, J. C., Eds. *Introduction to Zeolite Science and Practice*; Elsevier: Amsterdam, 1991.
- (3) Thomas, J. M. *Angew. Chem., Int. Ed. Engl.* **1994**, *33*, 913.
- (4) Thomas, J. M. *Angew. Chem., Int. Ed. Engl.* **1999**, *38*, 3588.
- (5) Cheetham, A. K.; Ferey, G.; Loiseau, T. *Angew. Chem., Int. Ed. Engl.* **1999**, *38*, 3268.
- (6) Haag, W. O.; Lago, R. M.; Weisz, P. B. *Nature* **1984**, *309*, 589.
- (7) Wright, P. A.; Thomas, J. M.; Cheetham, A. K.; Nowak, A. K. *Nature* **1985**, *318*, 611.
- (8) Derouane, E. G. *J. Catal.* **1986**, *100*, 541.
- (9) Derouane, E. G.; Vanderveken, D. J. *Appl. Catal.* **1988**, *45*, L15.
- (10) Raja, R.; Ratnasamy, P. *J. Mol. Catal.* **1995**, *100*, 93.
- (11) van Santen, R. A. *Catal. Technol.* **1998**, *2*, 161.
- (12) Jacobs, P. A.; Declerck, D. J.; Vandamme, L. J.; Uytterhoeven, J. B. *J. Chem. Soc., Faraday Trans. 1* **1975**, *71*, 1545.
- (13) Kwok, T. J.; Jayasuriya, K.; Damavarapu, R.; Brodman, B. W. *J. Org. Chem.* **1994**, *59*, 4939.
- (14) Bhaumik, A.; Tatsumi, T. *Chem. Commun.* **1998**, 463.
- (15) Wennerberg, J.; Ek, F.; Hansson, A.; Frejd, T. *J. Org. Chem.* **1999**, *64*, 54.
- (16) Hartmann, M.; Kevan, L. *Chem. Rev.* **1999**, *99*, 635.
- (17) Hirano, T.; Li, W.; Abrams, L.; Krusic, P. J.; Ottaviani, M. F.; Turro, N. J. *J. Org. Chem.* **2000**, *65*, 1319.
- (18) Turro, N. J.; Lei, X. G.; Li, W.; Liu, Z. Q.; McDermott, A.; Ottaviani, M. F.; Abrams, L. *J. Am. Chem. Soc.* **2000**, *122*, 11649.
- (19) Turro, N. J. *Acc. Chem. Res.* **2000**, *33*, 637.
- (20) Lee, S.-O.; Sankar, G.; Kitchin, S. J.; Dugal, M.; Thomas, J. M.; Harris, K. D. M. *Catal. Lett.* **2001**, *73*, 91.
- (21) Meier, W. M.; Olson, D. H., Eds. *Atlas of Zeolite Structure Types*; Butterworths: Markham, Canada, 1987; p 64.
- (22) Thomas, J. M.; Raja, R.; Sankar, G.; Bell, R. G. *Nature* **1999**, *398*, 227.
- (23) Dugal, M.; Sankar, G.; Raja, R.; Thomas, J. M. *Angew. Chem., Int. Ed.* **2000**, *39*, 2310.
- (24) Molecule **P** can exist as different configurational isomers, depending on whether the methyl groups lie on the same face or opposite faces of the six-membered ring. In particular, there are two configurational isomers: [A] with all three methyl groups on the same face of the six-membered ring and [B] with two methyl groups on one face and one methyl group on the other face. In the case of [A], and assuming a chair conformation of the six-membered ring, there are two molecular conformations (triquatorial and triaxial), which may be interconverted by ring inversion. Similarly in the case of [B], there are two molecular conformations (equatorial-axial-axial and axial-equatorial-equatorial), which may be interconverted by ring inversion. It is clear that (either for an individual conformation or on averaging over the ring-inversion processes discussed above), in the case of [A], all methyl groups are equivalent, whereas, in the case of [B], there are two different methyl group environments with populations in a 2:1 ratio. The solid-state  $^{13}\text{C}$  NMR spectrum recorded for acetaldehyde/ferrierite (Figure 3) and the solution-state  $^1\text{H}$  and  $^{13}\text{C}$  NMR spectra recorded for the organic species extracted from the ferrierite indicate that all methyl groups in the molecules of **P** have the same average environment, implying that only isomer [A] is produced. For this isomer, the conformation (triquatorial) with all methyl groups in equatorial positions should be favored energetically, at least for the isolated molecule, and furthermore, this conformation of [A] should be lower in energy than any conformation of isomer [B]. We note that, as each step in the proposed reaction mechanism (Figure 5) from acetaldehyde to **P** can be regarded as an equilibrium, it is reasonable to find a situation in which only the thermodynamically most stable isomer of **P** is obtained (provided, of course, that the production of this isomer is compatible with the spatial constraints imposed on the reaction by the ferrierite host structure).
- (25) If we denote the numbers of moles of acetaldehyde and **P** present at any stage during the reaction as  $n_A$  and  $n_P$ , respectively, the integrated intensity of the peaks due to **P** in the solid-state  $^{13}\text{C}$  NMR spectrum, expressed as a fraction of the total integrated intensity of peaks in the spectrum (acetaldehyde plus **P**), is:  $R = (3n_P)/(3n_P + n_A)$ . In deriving this equation, we recognize that, for a molecule of acetaldehyde, each peak in the spectrum represents a single  $^{13}\text{C}$  nucleus, whereas, for a molecule of **P**, each peak in the spectrum represents three equivalent  $^{13}\text{C}$  nuclei. Similar arguments hold for integration of the solution-state  $^1\text{H}$  NMR spectrum. Given the stoichiometry of the reaction (acetaldehyde  $\rightarrow$   $1/3$ **P**), the number of moles of acetaldehyde that have been consumed at any stage during the reaction is equal to three times the number of moles of **P** that have been produced. Thus, the percentage conversion is the following:  $C = 100$  (number of moles of acetaldehyde consumed)/(number of moles of acetaldehyde present initially) =  $100(3n_P)/(3n_P + n_A) = 100R$ . Rearrangement of this equation gives the molar ratio:  $n_P/n_A = R/(3 - 3R)$ .